

Deciphering a Nanocarbon-Based Artificial Peroxidase: Chemical Identification of the Catalytically Active and Substrate-Binding Sites on Graphene Quantum Dots**

Hanjun Sun, Andong Zhao, Nan Gao, Kai Li, Jinsong Ren, and Xiaogang Qu*

Abstract: The design and construction of efficient artificial enzymes is highly desirable. Recent studies have demonstrated that a series of carbon nanomaterials possess intrinsic peroxidase activity. Among them, graphene quantum dots (GQDs) have a high enzymatic activity. However, the catalytic mechanism remains unclear. Therefore, in this report, we chose to decipher their peroxidase activity. By selectively deactivating the ketonic carbonyl, carboxylic, or hydroxy groups and investigating the catalytic activities of these GQD derivatives, we obtained evidence that the C=O groups were the catalytically active sites, whereas the O=C-O- groups acted as substrate-binding sites, and -C-OH groups can inhibit the activity. These results were corroborated by theoretical studies. This work should not only enhance our understanding of nanocarbon-based artificial enzymes, but also facilitate the design and construction of other types of target-specific artificial enzymes.

Nanomaterials with similar functions to those of proteins are regarded as an important class of protein mimics and expected to substitute natural proteins in practical applications.^[1] Carbon nanomaterials have shown excellent catalytic activity in several important chemical and biochemical reactions.^[2] Interestingly, they are even regarded as nanozymes because they possess intrinsic enzymatic activity.^[2c] As nanozymes, carbon nanomaterials have advantages over natural enzymes, such as low costs, facile production on large scale, the possibility of long-term storage, and high stability in harsh environments.^[2c] Our group was the first to report the peroxidase-like activity of graphene oxide (GO),^[3] and has since focused on expanding the applications of GO, graphene nanocomposites, carbon nanotubes (CNTs), carbon dots (CDs), and graphene quantum dots (GQDs) as peroxidase-like catalysts.^[2c,4] Although the above-mentioned carbon nanozymes have exhibited enzymatic activity in

diagnostics and therapeutic applications, compared with natural peroxidase, the low efficiency of the carbon nanomaterials has unfortunately restricted their further applications.^[2b,c] Understanding their catalytic mechanism should facilitate the design and synthesis of more effective carbon nanozymes.^[2c,3,4]

GQDs, which can be regarded as small pieces of graphene, are a type of zero-dimensional material with characteristics derived from both graphene and CDs.^[5] Aside from some superior fluorescence properties, such as higher photostability against photobleaching and blinking than organic dyes and semiconductor quantum dots, GQDs exhibit a higher peroxidase-like activity than GO.^[4,6] Furthermore, GQDs display no apparent toxicity in vitro and in vivo, which should render them applicable in the area of biomedicine.^[7] For these reasons, GQDs have attracted significant attention from researchers in both material and biological science. Recently, we have found that the peroxidase-like activity of GQDs stems from their ability to catalyze the decomposition of H_2O_2 , generating HO^\bullet .^[4] However, the catalytic and substrate-binding sites of GQDs acting as nano-peroxidases are unknown. Herein, through selectively deactivating these specific oxygen-containing functional groups^[8] and investigating the catalytic activity of different GQD derivatives as peroxidase mimics, we obtained evidence that the ketonic carbonyl groups (-C=O) are the catalytically active sites, whereas the carboxylic groups (O=C-O-) act as substrate-binding sites, and the hydroxy groups (-C-OH) can even inhibit the catalytic reaction. For the first time, we clarify the different functions of these three kinds of typical oxygen functional groups on the surface of GQDs in catalytic peroxidase-like reactions, which reflects the intrinsic catalytic activity of GQDs as a peroxidase mimic.

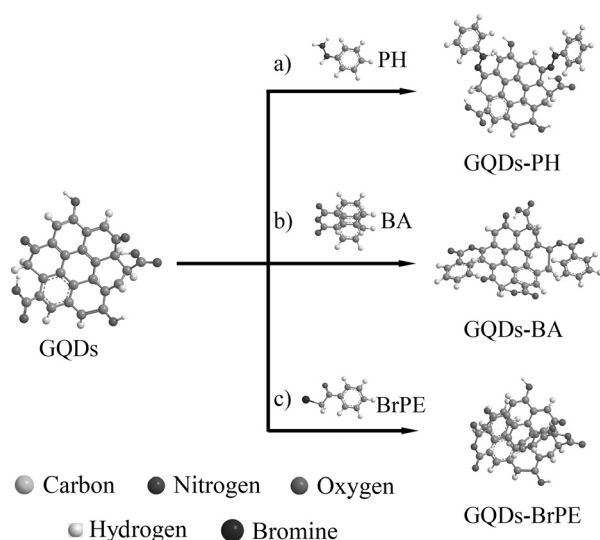
The GQDs were synthesized according to previous reports.^[4,9] The as-prepared GQDs were mainly covered with carbonyl, carboxylic, and hydroxy groups on their surface.^[4,9] Phenylhydrazine (PH), benzoic anhydride (BA), and 2-bromo-1-phenylethanone (BrPE) were chosen as the titrants to specifically react with the ketonic carbonyl, hydroxy, and carboxylic groups on the GQDs, respectively (Scheme 1), because these reactions have been shown to be highly specific under gentle reaction conditions.^[8] The typical transmission electron microscopy (TEM) and atomic force microscopy (AFM) images of GQDs and the as-prepared GQD derivatives (referred to as GQDs-PH, GQDs-BA, and GQDs-BrPE) demonstrated that the reactions with PH, BA, and BrPE did not change the average sizes and heights as well as the relative size and height distributions of the GQD derivatives compared with the unmodified GQDs (Support-

[*] H. Sun, A. Zhao, Dr. N. Gao, Dr. K. Li, Prof. J. Ren, Prof. X. Qu
Laboratory of Chemical Biology and State Key Laboratory of Rare
Earth Resource Utilization, Changchun Institute of Applied
Chemistry, Chinese Academy of Sciences
Changchun, Jilin 130022 (China)
E-mail: xqu@ciac.ac.cn

H. Sun, A. Zhao
University of Chinese Academy of Science
Beijing, 100039 (China)

[**] This work was supported by the 973 Project (2011CB936004, 2012CB720602), and the NSFC (21210002, 21431007, 91413111, 21402183).

Supporting information for this article is available on the WWW under <http://dx.doi.org/10.1002/anie.201500626>.



Scheme 1. The chemical titration processes for a) ketonic carbonyl, b) hydroxy, and c) carboxylic groups on GQDs.

ing Information, Figures S1 and S2). Owing the different surface states, the changes observed in the photoluminescence (PL) and UV spectra of the GQD derivatives compared with those of the parent GQDs indicate that the titration reactions have indeed occurred (Figures S3 and S4).^[9b,c,10]

Fourier transform infrared (FT-IR) spectroscopy, zeta potential measurements, nuclear magnetic resonance (NMR) spectroscopy, and X-ray photoelectron spectroscopy (XPS) were used to study the surface groups of the GQDs. The FT-IR spectrum of GQDs-PH showed an obvious vibration band at 1840 cm^{-1} , which is due to the formation of C=N bonds during titration (Figure S5).^[8] For the GQDs-BA, an increase in intensity of the peak corresponding to the ester group at 1730 cm^{-1} was observed, whereas the intensities of the C-H stretching vibrations at 2924 cm^{-1} and 2850 cm^{-1} , which are due to the BrPE substituents, were enhanced for the GQDs-BrPE (Figure S5).^[11] Especially for the GQDs-BrPE, compared with other GQDs, the obvious decrease in the zeta potential value indicated the removal of O=C-O- moieties by BrPE (pH 7.0, Figure S6). Furthermore, the peak area obtained through deconvolution of the O 1s XPS spectra could reflect the relative surface concentration of different O species and the extent of the three titration reactions.^[8,12] As displayed in the O 1s XPS spectra (Figure 1a), the decreases in the intensities of the C=O signal for the GQDs-PH and of the C-OH signal for the GQDs-BA and the increase in the C=O signal for the GQDs-BrPE also indicated that the three reactions had occurred, which is consistent with the results of the FT-IR, zeta potential, and NMR measurements (Figures S5–S7). By integrating the relative peak areas, we determined that the surface concentrations of C=O (ketonic carbonyl groups), C-OH (phenol and alcohol groups), and O=C-O- groups (carboxylic groups) on the GQDs dropped by approximately 92, 93, and 98 % after the reactions with PH, BA, and BrPE, respectively. Furthermore, the N 1s XPS spectrum of the GQDs-PH showed a significant peak that is due to the formation of C=N bonds (Figure 1b).^[8] As determined by XPS, the GQDs-

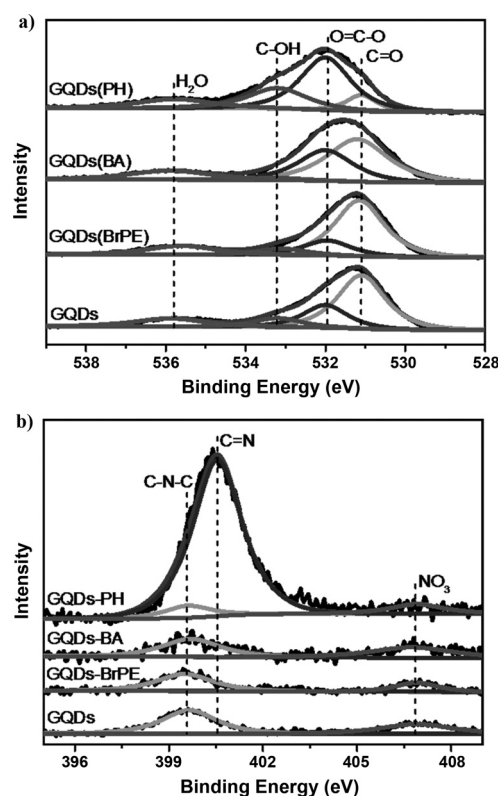


Figure 1. a) O 1s and b) N 1s XPS spectra of GQDs-PH, GQDs-BA, GQDs-BrPE, and GQDs.

PH had a nitrogen content of 9.9% (atomic percent), compared with a nitrogen content of 4.6% in the parent GQDs.

The oxidation reaction of 2,2'-azinobis(3-ethylbenzthiazoline-6-sulfonate) (ABTS) in the presence of H_2O_2 was selected as a model reaction to evaluate the peroxidase-like activity of the GQDs and their derivatives (GQDs-PH, GQDs-BA, and GQDs-BrPE) by monitoring the change in the ABTS absorption at 417 nm .^[4] The contributions of the oxygen functional groups (C=O , C-OH , and O=C-O-) to the catalytic oxidation reaction could be evaluated by comparing the enzymatic activity of the unmodified GQDs with those of the GQD derivatives. According to the data shown in Figure S8, for both the parent GQDs and the three derivatives, the optimal conditions were found to be pH 4.0 and approximately 37°C .^[4] As shown in Figure 2, under these conditions, the GQDs-BA showed the highest enzymatic activity among the four different GQDs whereas the activity of the GQDs-PH was much lower than that of the GQDs, and the catalytic activity of the GQDs-BrPE was almost the same as that of the parent GQDs, indicating that the enzymatic activity of the GQDs was related to the oxygen functional groups and that the C=O groups might play a very important role in the catalytic process.

To further analyze the functions of the oxygen functional groups in the catalytic reaction under our experimental conditions, we used the Michaelis–Menten model to analyze and compare the kinetic parameters of the GQDs and their derivatives. From Lineweaver–Burk plots, values for the

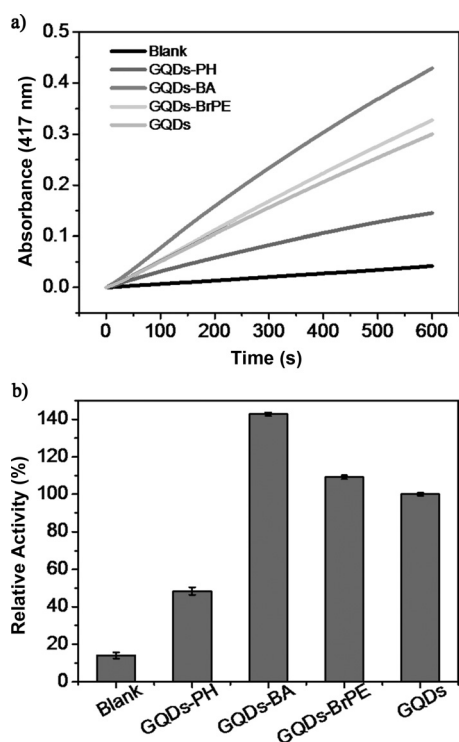


Figure 2. Comparison of the peroxidase-like activities of the parent GQDs and GQD derivatives. a) The time dependence of the absorbance at 417 nm. b) The absorbance at 417 nm after a 10 min enzymatic reaction with GQDs-PH, GQDs-BA, GQDs-BrPE, or GQDs. Experiments were carried out using GQDs or GQD derivatives ($40 \mu\text{g mL}^{-1}$) in a reaction volume of 0.5 mL in Na_2HPO_4 buffer (25 mM, pH 4.0) and H_2O_2 (50 mM) with ABTS (2.5 mM) as the substrate.

maximum initial velocity (V_{max}) and the Michaelis–Menten constant (K_m) were obtained (Figure S9), which are summarized in Table 1.^[3,13] The K_m value is a measure of the binding affinity between enzymes and substrates, and the V_{max} value reveals the turnover number of enzymes, which reflects their catalytic activity.^[14] With ABTS as the substrate, there were no significant differences between the V_{max} values of the parent GQDs and the different GQD derivatives. However, the observed increase in the K_m value for the GQD derivatives implied that the removal of oxygen functional groups (especially of $-\text{C}=\text{O}$) reduced the affinity between the GQDs and ABTS, suggesting that the oxygen functional groups played a role on enrichment of ABTS on the surface of GQDs

Table 1: Comparison of the apparent Michaelis–Menten constants (K_m) and maximum reaction rates (V_{max}) of GQD derivatives and GQDs.

Catalyst	Substrate	K_m [mM]	V_{max} [$\times 10^{-8} \text{ M s}^{-1}$]
GQDs-PH	H_2O_2	1.09 ± 0.03	0.211 ± 0.008
GQDs-BA	H_2O_2	1.12 ± 0.02	2.67 ± 0.02
GQDs-BrPE	H_2O_2	7.94 ± 0.01	10.55 ± 0.02
GQDs	H_2O_2	1.17 ± 0.03	1.24 ± 0.04
GQDs-PH	ABTS	681.3 ± 2.1	1.27 ± 0.02
GQDs-BA	ABTS	21.4 ± 0.3	2.14 ± 0.02
GQDs-BrPE	ABTS	64.7 ± 0.2	2.33 ± 0.03
GQDs	ABTS	10.4 ± 0.1	1.78 ± 0.05

in this enzymatic reaction. With H_2O_2 as the substrate, the K_m value of the GQDs-BrPE was significantly higher than those of the GQDs, GQDs-PH, and GQDs-BA. This finding indicates that the removal of $\text{O}=\text{C}-\text{O}-$ groups reduces the affinity between the GQDs and H_2O_2 , and that the $\text{O}=\text{C}-\text{O}-$ groups could be the binding sites for H_2O_2 . Furthermore, the V_{max} value of the GQDs-PH was much lower than those of the GQDs, GQDs-BA, and GQDs-BrPE, indicating that the $-\text{C}=\text{O}$ groups were the catalytic sites for H_2O_2 decomposition. It should be pointed out that the GQDs-BrPE had the largest V_{max} value with H_2O_2 as the substrate, which could be attributed to the fact that when the $\text{O}=\text{C}-\text{O}-$ groups are removed by reaction with BrPE, the $-\text{C}=\text{O}$ groups of the BrPE that are now located on the surface of the GQDs can act as catalytic sites for H_2O_2 decomposition. Meanwhile, the removal of $\text{O}=\text{C}-\text{O}-$ groups reduced the number of binding sites for H_2O_2 on the GQDs; therefore, the GQDs-BrPE did not show the highest enzymatic activity. Furthermore, the V_{max} value of the GQDs-BA was approximately two times larger than that of the GQDs whereas their K_m values were similar, which might be due to the fact that the BA had reacted with the $-\text{C}-\text{OH}$ groups, thus reducing the possibility that generated HO^\bullet radicals are trapped by alcoholic or phenolic hydroxy groups on the GQDs; the GQDs-BA thus have the highest catalytic activity.^[15] Furthermore, according to the Arrhenius equation,^[16] from linear fitting of the logarithmic plots of the reaction rates against the reciprocal of the reaction temperature (290–330 K; Figure S10), the activation energies were estimated to be 47.0 ± 0.5 , 41.5 ± 0.4 , 44.3 ± 0.4 , and $44.7 \pm 0.5 \text{ kJ mol}^{-1}$ for the GQDs-PH, GQDs-BA, GQDs-BrPE, and GQDs at pH 4.0 (25 mM PBS buffer), respectively, whereas an activation energy of $49.5 \pm 0.5 \text{ kJ mol}^{-1}$ was determined for the reaction without any catalysts. The data on the activation energies show that these four GQDs can reduce the energy barrier and are catalytically active. As the GQDs-BA had the lowest activation energy, and the GQDs-PH had a larger activation energy than the GQDs, the $-\text{C}=\text{O}$ groups were determined to be the catalytically active sites, and the existence of $-\text{C}-\text{OH}$ groups was found to decrease the catalytic activity of the GQDs.

Considering that the peroxidase-like activity of GQDs originates from their ability to catalyze the decomposition of H_2O_2 to generate hydroxyl radicals (HO^\bullet), fluorescence experiments were carried out to monitor HO^\bullet production during the interaction between the GQD derivatives and H_2O_2 .^[4] The fluorescence probe, terephthalic acid (TA), was used for tracking of HO^\bullet because it can capture HO^\bullet and generate 2-hydroxyterephthalic acid (TAOH), which emits unique fluorescence at approximately 435 nm (Figure 3a), to study the ability of the parent GQDs and their derivatives to convert H_2O_2 into HO^\bullet radicals.^[4,17] The changes in the fluorescence spectra of solutions containing GQD derivatives, TA, and H_2O_2 are shown in Figure 3b–f. After 24 hours, a remarkable fluorescence enhancement at 435 nm indicated the presence of HO^\bullet radicals compared with control experiments without a catalyst, confirming that the GQDs and their derivatives could convert H_2O_2 into HO^\bullet and thus exhibit peroxidase-like activity.^[4] Among the four different GQDs, the GQDs-PH had the lowest ability to produce HO^\bullet radicals,

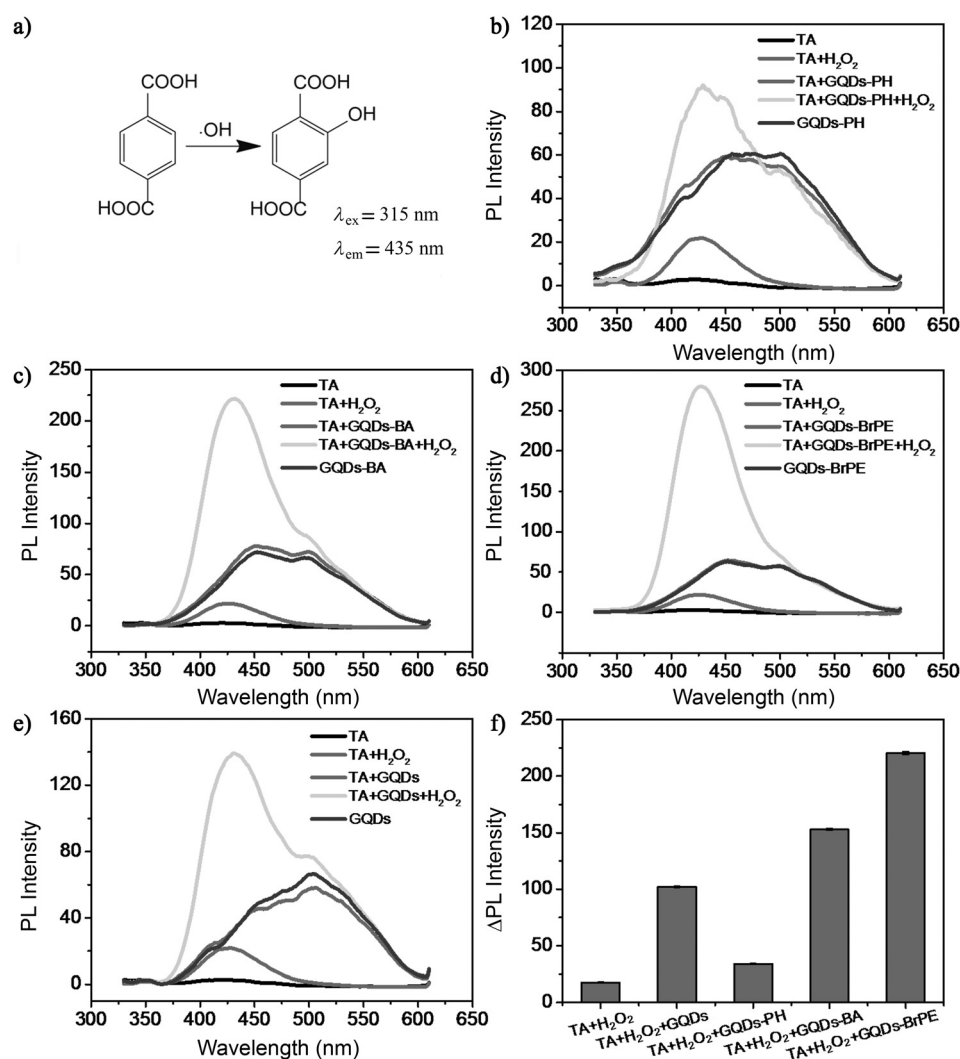


Figure 3. a) The reaction between a hydroxyl radical and terephthalic acid (TA). b–e) Fluorescence spectra of weakly acidic PBS solutions (pH 6.0, 25 mM) containing only TA, TA and H_2O_2 , only GQD derivatives or GQDs, TA and GQD derivatives or GQDs, or TA and GQD derivatives or GQDs and H_2O_2 after a reaction time of 24 hours. The TA, H_2O_2 , and GQDs concentrations were 0.5 mM, 1 mM, and $100 \mu\text{g mL}^{-1}$, respectively. f) Histograms of the changes in photoluminescence intensity (ΔPL) show the catalytic effect of the GQD derivatives or GQDs; error bars are taken from three parallel experiments.

which is consistent with the results of the enzymatic activity measurements and demonstrated that the ketonic $-\text{C}=\text{O}$ groups were the catalytic sites for HO^\bullet production (Figure 3b,f). As the GQDs-BA showed a higher activity in converting H_2O_2 into HO^\bullet than the GQDs, indicating that the removal of $-\text{C}-\text{OH}$ groups improved conversion, the $-\text{C}-\text{OH}$ groups on the GQDs inhibited this catalytic reaction (Figure 3c,f). Furthermore, even the GQDs-BrPE did not show a higher peroxidase-like activity than the GQDs and GQDs-BA as the amount of HO^\bullet generated from the GQDs-BrPE was larger than for the GQDs and GQDs-BA, which is consistent with the V_{max} values of these four GQD variants (Figure 3d,f). In short, the results of the fluorescence experiments also confirmed that as a peroxidase mimic, GQDs have catalytic sites ($-\text{C}=\text{O}$) and substrate-binding sites ($\text{O}=\text{C}-\text{O}-$) like natural enzymes. Furthermore, $-\text{C}-\text{OH}$ groups could decrease the enzymatic activity of GQDs.

a higher catalytic activity for H_2O_2 decomposition than the $-\text{COOH}$ moieties, which corroborated the experimental results that the $-\text{C}=\text{O}$ groups act as the catalytic sites. Moreover, owing to the stronger hydrogen bond interaction, the binding energy (E_b) of H_2O_2 on $-\text{COOH}$ groups (-0.67 eV) was lower than that for the $-\text{C}=\text{O}$ (-0.30 eV) and $-\text{C}-\text{OH}$ groups (-0.17 eV), which also supports our experimental result that the $-\text{COOH}$ groups act as the binding sites for H_2O_2 (Figure S12).

In summary, we have synthesized three GQD derivatives through chemical reactions between GQDs and PH, BA, and BrPE as the selective deactivation agents to specifically react with the ketonic carbonyl, hydroxy, and carboxyl groups on the GQDs, respectively. By measuring the enzyme kinetic parameters of different GQDs and conducting a theoretical study, we found that the $-\text{C}=\text{O}$ groups act as the catalytically active sites and the $\text{O}=\text{C}-\text{O}-$ groups serve as the substrate-

A theoretical study provided further evidence on the catalytic mechanism, consolidating our experimental results. The mechanisms of H_2O_2 dissociation and HO^\bullet formation on $-\text{C}=\text{O}$ and $-\text{COOH}$ groups were investigated by theoretical calculations using the Vienna ab initio simulation package (VASP),^[18] and the energy barriers (ΔE) and reaction energies (ΔH) were determined. The computational details are shown in the Supporting Information. For the $-\text{C}=\text{O}$ groups, the rate-determining step was determined to be attack of H_2O_2 on the $\text{C}=\text{O}$ double bond (**S1**) with formation of intermediate **S2** ($\Delta E = 0.90 \text{ eV}$, $\Delta H = -0.14 \text{ eV}$; Figure S11 a). Then, intermediate **S2** readily dissociates into HO^\bullet and $-\text{C}=\text{O}$ readily owing to the low barrier (0.09 eV) and high exothermicity (-4.20 eV). For the $-\text{COOH}$ groups,^[19] as shown in Figure S11 b, H_2O_2 attacked the $-\text{C}=\text{O}$ double bond (**S1'**) of $-\text{COOH}$ to form intermediate **S2'**. Then, a water molecule was eliminated from **S2'** to yield **S3'**. Finally, intermediate **S3'** dissociates to **S4'** forming HO^\bullet radicals. The rate-determining step was the conversion of **S2'** into **S3'** with an energy barrier of 1.45 eV , which is higher than that of the corresponding reaction on $-\text{C}=\text{O}$ groups (0.90 eV). Thus, the $-\text{C}=\text{O}$ groups show

binding sites. The existence of $-C-OH$ groups decreases the catalytic activity of GQDs. The clarification of the different functions of the oxygen functional groups ($-C=O$, $-C-OH$, and $O=C-O-$) typically found on the surface of GQDs in catalytic peroxidase-like reactions further enhances our understanding of the intrinsic enzymatic activity of GQDs. We hope that this work has not only provided new insights into deciphering nanocarbon-based artificial enzymes, but will also facilitate the design and construction of other types of target-specific artificial enzymes.

Keywords: catalysis · graphene quantum dots · nanoparticles · peroxidase activity · reaction mechanisms

How to cite: *Angew. Chem. Int. Ed.* **2015**, *54*, 7176–7180
Angew. Chem. **2015**, *127*, 7282–7286

-
- [1] N. A. Kotov, *Science* **2010**, *330*, 188–189.
- [2] a) D. S. Su, S. Perathoner, G. Centi, *Chem. Rev.* **2013**, *113*, 5782–5816; b) H. Wei, E. K. Wang, *Chem. Soc. Rev.* **2013**, *42*, 6060–6093; c) Y. Lin, J. Ren, X. Qu, *Acc. Chem. Res.* **2014**, *47*, 1097–1105.
- [3] Y. Song, K. Qu, C. Zhao, J. Ren, X. Qu, *Adv. Mater.* **2010**, *22*, 2206–2210.
- [4] H. Sun, N. Gao, K. Dong, J. Ren, X. Qu, *ACS Nano* **2014**, *8*, 6202–6210.
- [5] a) L. L. Li, G. H. Wu, G. H. Yang, J. Peng, J. W. Zhao, J. J. Zhu, *Nanoscale* **2013**, *5*, 4015–4039; b) H. Sun, L. Wu, W. Wei, X. Qu, *Mater. Today* **2013**, *16*, 433–442.
- [6] Y. Zhang, C. Y. Wu, X. J. Zhou, X. C. Wu, Y. Q. Yang, H. X. Wu, S. W. Guo, J. Y. Zhang, *Nanoscale* **2013**, *5*, 1816–1819.
- [7] a) M. Nurunnabi, Z. Khatun, K. M. Huh, S. Y. Park, D. Y. Lee, K. J. Cho, Y. K. Lee, *ACS Nano* **2013**, *7*, 6858–6867; b) C. Y. Wu, C. Wang, T. Han, X. J. Zhou, S. W. Guo, J. Y. Zhang, *Adv. Healthcare Mater.* **2013**, *2*, 1613–1619; c) Y. Chong, Y. F. Ma, H. Shen, X. L. Tu, X. Zhou, J. Y. Xu, J. W. Dai, S. J. Fan, Z. J. Zhang, *Biomaterials* **2014**, *35*, 5041–5048.
- [8] W. Qi, W. Liu, B. S. Zhang, X. M. Gu, X. L. Guo, D. S. Su, *Angew. Chem. Int. Ed.* **2013**, *52*, 14224–14228; *Angew. Chem.* **2013**, *125*, 14474–14478.
- [9] a) L. L. Li, J. Ji, R. Fei, C. Z. Wang, Q. Lu, J. R. Zhang, L. P. Jiang, J. J. Zhu, *Adv. Funct. Mater.* **2012**, *22*, 2971–2979; b) H. Sun, N. Gao, L. Wu, J. Ren, W. L. Wei, X. G. Qu, *Chem-Eur. J.* **2013**, *19*, 13362–13368; c) H. Sun, L. Wu, N. Gao, J. Ren, X. Qu, *ACS Appl. Mater. Interfaces* **2013**, *5*, 1174–1179.
- [10] H. Z. Zheng, Q. L. Wang, Y. J. Long, H. J. Zhang, X. X. Huang, R. Zhu, *Chem. Commun.* **2011**, *47*, 10650–10652.
- [11] N. B. Colthup, L. H. Day, S. E. Wiberley, *Introduction to Infrared and Raman Spectroscopy*, 3rd ed., Academic Press, San Diego, **1990**.
- [12] a) T. I. T. Okpalugo, P. Papakonstantinou, H. Murphy, J. McLaughlin, N. M. D. Brown, *Carbon* **2005**, *43*, 153–161; b) S. Kundu, Y. M. Wang, W. Xia, M. Muhler, *J. Phys. Chem. C* **2008**, *112*, 16869–16878.
- [13] L. Z. Gao, J. Zhuang, L. Nie, J. B. Zhang, Y. Zhang, N. Gu, T. H. Wang, J. Feng, D. L. Yang, S. Perrett, X. Yan, *Nat. Nanotechnol.* **2007**, *2*, 577–583.
- [14] J. M. Berg, J. L. Tymoczko, L. Stryer, *Biochemistry*, 5th ed., W. H. Freeman, **2002**.
- [15] a) M. R. Billany, K. Khatib, M. Gordon, J. K. Sugden, *Int. J. Pharm.* **1996**, *137*, 143–147; b) B. Lipinski, *Oxid. Med. Cell. Longevity* **2011**, 809696.
- [16] M. Menzinger, R. Wolfgang, *Angew. Chem. Int. Ed. Engl.* **1969**, *8*, 438–444; *Angew. Chem.* **1969**, *81*, 446–452.
- [17] a) K. Ishibashi, A. Fujishima, T. Watanabe, K. Hashimoto, *Electrochem. Commun.* **2000**, *2*, 207–210; b) S. G. Ge, F. Liu, W. Y. Liu, M. Yan, X. R. Song, J. H. Yu, *Chem. Commun.* **2014**, *50*, 475–477.
- [18] a) G. Kresse, J. Hafner, *Phys. Rev. B* **1993**, *47*, 558–561; b) G. Kresse, J. Hafner, *Phys. Rev. B* **1994**, *49*, 14251–14269; c) G. Kresse, J. Furthmuller, *Comp. Mater. Sci.* **1996**, *6*, 15–50; d) G. Kresse, J. Furthmuller, *Phys. Rev. B* **1996**, *54*, 11169–11186.
- [19] R. Zhao, X. Zhao, X. Gao, *Chem. Eur. J.* **2015**, *21*, 960–964.

Received: January 22, 2015

Revised: March 9, 2015

Published online: May 4, 2015